electrons is very small. Studies in neon-argon (1000:1) mixtures yield similar results, in that the electron density decay curves are accurately exponential in character, and thus are not at all consistent with the recombination decay curves, Eq. 4, observed in pure argon.

V. SUMMARY AND DISCUSSION

The present paper has presented experimental evidence that electron-ion recombination is an important electron removal process in ionized noble gases such as neon and argon. It has been shown that the decay of electron density with time during the afterglow following a discharge follows a volume recombination law, and that this decay is accompanied by a persistent emission of radiation from the volume of the ionized gas. If this radiation is attributed to the formation of excited atoms during the recombination process, then the absolute intensity of the afterglow radiation is consistent with the large recombination coefficients, $10^{-7}<\alpha<10^{-6}$ cc/sec, deduced from the measured electron-density decay curves. It is also shown that the afterglow radiation can be decreased by momentarily increasing the electron energy—consistent with the expectation that the rate of electron-ion recombination decreases with increasing electron energy.

Finally, the mechanism of the recombination process is investigated by comparing the electron decay curves under conditions in which first molecular ions and then atomic ions are expected to predominate during the afterglow. If dissociative recombination, Eq. 2, provides the efficient capture mechanism required to explain the large α values, it can only take place when molecular ions are present. It is shown that, under conditions when Ar_2^+ ions predominate, a large recombination loss of electrons is observed, while when Ar^+ ions are expected to predominate, only ambipolar diffusion loss of electrons and ions can be detected.

A second, more conclusive proof of the hypothesis that dissociative recombination is the process responsible for the large α values observed experimentally would be provided by detection of the kinetic energy of the dissociating atoms produced by the recombination event.[30] In part II of this paper we present the detailed results of experiments designed to detect the dissociation kinetic energy of the atoms produced during recombination in helium afterglows.

The author wishes to express his gratitude to T. Holstein for important contributions and stimulating discussions during the course of these experiments.

[30] M. A. Biondi, Phys. Rev. **93**, 650A (1954), W. A. Rogers and M. A. Biondi, Bull. Am. Phys. Soc. **2**, 87 (1957).

PHYSICAL REVIEW VOLUME 129, NUMBER 3 1 FEBRUARY 1963

Nuclear Quadrupole Interaction of Sb^{121} and Sb^{123} in Antimony Metal*

R. R. HEWITT AND B. F. WILLIAMS†
Department of Physics, University of California, Riverside California,
(Received 20 August 1962)

The five nuclear quadrupole resonances of Sb^{121} and Sb^{123} have been measured at 4.2°K giving the quadrupole couplings $eqQ=76.867\pm0.001$ and 97.999 ± 0.001 Mc/sec, respectively. The temperature dependence of the interaction has been measured from 2 to 480°K. Both isotopes have the same temperature dependence of $(1/\nu)(d\nu/dT)\approx2.4\times10^{-4}$ °K^{-1}. The ionic field gradient provides about 10% of this measured quadrupole coupling.

I. THE NUCLEAR ELECTROSTATIC INTERACTION WITH ITS ENVIRONMENT

THE general electrostatic interaction between a nucleus and those charge distributions external to that nucleus is

$$H=\int_{\tau_e}\int_{\tau_n}(\rho_n\rho_e/r_{en}-r_{en})d\tau_n d\tau_e \qquad (1)$$

where ρ_n is the charge density within the nucleus and ρ_e is the charge density external to the volume of the nucleus. This interaction may be written[1] as an expansion with respect to the charge centroid of the nucleus

$$H_k=\frac{4\pi}{2k+1}\sum_{q=-k}^{k}\int_{\tau_n}\rho_n r_n{}^k Y_q{}^{(k)}(\cos\theta_n,\varphi_n)d\tau_n \cdot\int_{\tau_e}\rho_e r_e{}^{-(k+1)}Y_{-q}{}^{(k)}(\cos\theta_e,\varphi_e)d\tau_e, \qquad (2)$$

where $Y_q{}^{(k)}$ are normalized tesseral harmonics and the dot indicates a tensor scalar product of degree k. The $k=0$ term is independent of orientation and not of direct

* Work supported in part by the National Science Foundation and the Research Corporation.
† National Science Foundation Cooperative Graduate Fellow.

[1] N. F. Ramsey, *Molecular Beams* (Clarendon Press, Oxford 1956).

interest here. All odd k have zero contribution under the assumption of the conservation of the parity of the ground-state nuclear eigenfunctions; no electric moments of odd k have been reported for these ground states. Of the remaining terms in this expansion the first two, $k=2$ and $k=4$, are the quadrupole and hexadecapole interactions. The energy levels associated with the orientation of these classical energy terms may be calculated in an (I,m) representation,[2,3] remembering that the axis of quantization is the spin axis, I, of the nucleus. In the case of axial symmetry for the external charge distributions the energy levels for the quadrupole interactions are

$$H_2=[eqQ/4I(2I-1)][3m^2-I(I+1)]. \tag{3}$$

where

$$eQ=\int_{\tau_n}\psi_{I,I}{}^*\rho_n(r_n)(3z_n{}^2-r_n{}^2)\psi_{I,I}d\tau_n,$$

and

$$q=\int_{\tau_e}[(3\cos^2\theta_e-1)/r_e{}^2]\rho_e d\tau_e.$$

The energy levels for hexadecapole interactions are

$$H_4=\frac{ehH[35m^4-30m^2I(I+1)+25m^2+3I^2(I+1)^2-6I(I+1)]}{128I(I-1)(2I-1)(2I-3)},$$

where

$$eH=\int_{\tau_n}\psi_{I,I}{}^*r_n{}^4(35\cos^4\theta_n-30\cos^2\theta_n+3)\psi_{I,I}d\tau_n, \tag{4}$$

and

$$h=\int_{\tau_e}\frac{\rho_e(r_e)(35\cos^4\theta_e-30\cos^2\theta_e+3)d\tau_e}{r_e{}^5}.$$

The charges external to the nucleus are usually separated into several elements:

1. The ion core is a closed shell and if undistorted will provide no contribution to q or h; however, the presence of other charges does produce a distortion of the ion core and its effect is included as the Sternheimer antishielding factor in each relation.[4-6]

$$q\rightarrow(1-\gamma_\infty)q_0,$$

and

$$h\rightarrow(1-\eta_\infty)h_0, \tag{5}$$

where the 0 subscript indicates the value at the ion site. These polarizability effects are assumed to be properties of the ground-state ion core electrons and are not to depend on the nature of the source of q_0 and h_0.

2. The other ions of the lattice may be represented as an array of monopole charges and higher induced moments. If the ion is at electric equilibrium, the induced dipole will not exist; q for induced quadrupole moments has been calculated for tetragonal lattices.[7]

3. The last contributor is the extra-ionic electrons. It is the spatial distribution of these electrons that is usually the unknown element in this interaction. The nuclear quadrupole resonance study, of which this work is a part, has been extended in metals in order to obtain more information about the spatial distribution of these extra-ionic electrons in metal environments. The directions of interpretation of the interactions in antimony metal are discussed in the last section of this paper.

II. EXPERIMENTAL METHOD

The nuclear resonance measurements were made with a variable frequency marginal oscillator similar to the Pound-Knight[8] oscillator. The resonance was modulated with an on-off magnetic square wave of about 100-Oe amplitude. The modulated signal was detected with a narrow-band, phase-sensitive detector and displayed on a recording potentiometer.

Frequency measurements were made by continuously monitoring with a Hewlett-Packard model 524C electronic counter that was calibrated against WWV. All frequency markers were made with a precision of ± 50 cps.

The samples were 325-mesh metal powder prepared from zone-refined antimony supplied by the Consolidated Mining and Smelting Company of Canada; it has a reported impurity of arsenic of less than 2 ppm. Annealing was done in a carbon boat under a vacuum of 5×10^{-5} mm of Hg and the powder was then sieved through a 325-mesh screen to remove any resulting agglomerates. The metal powder was mixed with an equal volume of 325-mesh quartz powder for measurements below room temperature.

The sample was located in Pyrex Dewars for all the measurements. In the range of 4°K to ambient, the temperature was varied by cooling and making measurements as the sample warmed to room temperature. The temperature was monitored by a thermocouple inserted in the metal powder sample. Below liquid nitrogen temperature, a Au-Co vs Ag-Au thermocouple was used;

[2] E. U. Condon and G. H. Shortley, *Theory of Atomic Spectra* (Cambridge University Press, Cambridge, England, 1935).
[3] The mathematical methods used in this development are shown by G. Racah, Phys. Rev. **62**, 438 (1942).
[4] T. P. Das and R. Bershohn, Phys. Rev. **102**, 733 (1956).
[5] R. M. Sternheimer, Phys. Rev. Letters **6**, 190 (1961).
[6] R. M. Sternheimer, Phys. Rev. **123**, 870 (1961).
[7] T. T. Taylor, Phys. Rev. **127**, 120 (1962).
[8] R. V. Pound and W. D. Knight, Rev. Sci. Instr. **21**, 219 (1950).

at all higher temperatures, a copper-constantan thermocouple was used. For measurements above room temperature, a bifilar heater wire was wound around the outside of the rf can. The temperatures are measured with a precision of ± 0.1°K. All data from the several runs of the temperature dependence are in good internal agreement and in agreement with the fixed temperature points taken at 78°K, −78.5°C, and 0°C.

III. RESONANCE FREQUENCIES AND LINEWIDTHS

The two stable isotopes of antimony Sb^{121} and Sb^{123} have nuclear spins $\frac{5}{2}$ and $\frac{7}{2}$,[9] magnetic moments 3.3417 and 2.5334,[10] quadrupole moments of -0.3 ± 0.2 and -1.2 ± 0.2,[11] and about an equal abundance of 57.25% and 42.75%, respectively. Antimony has a trigonal arsenic-type structure; the unit cell may be visualized as a body-centered cube elongated along a body diagonal and with the body-centered ion displaced slightly along this long-body diagonal, giving each ion three nearest neighbors and a threefold axis of symmetry along this [111] direction. This symmetry requires that the electric field gradient and the hexadecapole field be axially symmetric. From Eqs. (3) and (4), the energy levels shown in Table I are readily found. From the selection rules for the magnetic dipole interaction with the rf magnetic field, the $(|m|-1)\rightarrow|m|$ transitions provide the resonance frequencies shown in Table I.

TABLE I. Energy levels and resonance frequencies.

m	$H_2\times(eqQ)^{-1}$	$H_4\times(ehH)^{-1}$	$(\lvert m-1\rvert\rightarrow m)$
		Sb^{121}	
$\frac{1}{2}$	$-\frac{4}{20}$	$+\frac{2}{64}$	
			$\frac{3}{20}eqQ-\frac{5}{64}ehH$
$\frac{3}{2}$	$-\frac{1}{20}$	$-\frac{3}{64}$	
			$\frac{6}{20}eqQ+\frac{4}{64}ehH$
$\frac{5}{2}$	$+\frac{5}{20}$	$+\frac{1}{64}$	
		Sb^{123}	
$\frac{1}{2}$	$-\frac{5}{28}$	$+\frac{9}{448}$	
			$\frac{1}{14}eqQ-\frac{6}{224}ehH$
$\frac{3}{2}$	$-\frac{3}{28}$	$-\frac{3}{448}$	
			$\frac{2}{14}eqQ-\frac{5}{224}ehH$
$\frac{5}{2}$	$+\frac{1}{28}$	$-\frac{13}{448}$	
			$\frac{3}{14}eqQ+\frac{10}{224}ehH$
$\frac{7}{2}$	$+\frac{7}{28}$	$+\frac{7}{448}$	

Since annealing the sample has been found to affect both the resonance frequencies and the linewidths, it is necessary to describe these effects before proceeding with the description of the measurements. Before annealing, the only resonances observable were the $(\frac{1}{2}\rightarrow\frac{3}{2})$ transitions of the two isotopes. Annealing for 24 h at 350°C narrowed the $(\frac{1}{2}\rightarrow\frac{3}{2})$ resonance linewidths by about 50%, but the higher m-value transitions were still not observable. Annealing for 2 h at 560°C was sufficient for the observation of the other three transitions. However, annealing at a still higher temperature caused a shift in resonance frequencies of the $(\frac{1}{2}\rightarrow\frac{3}{2})$ transitions. The other three resonances did not change their resonance frequency or linewidth from this annealing. A summary of these results for the $(\frac{1}{2}\rightarrow\frac{3}{2})$ transitions is shown in Table II. The measured resonance frequencies and their linewidths are shown in Table III, where the uncertainty listed is the standard deviation from a number of measurements of each value. A comparison of the resonance frequencies in Table I and the measured frequencies in Table III provides the measure of eqQ and ehH shown at the bottom of Table III. The very small deviations in the resonance frequencies from a pure quadrupole interaction cannot be identified as hexadecapole interactions because of the frequency dependence on the annealing. This result leaves the $(\frac{1}{2}\rightarrow\frac{3}{2})$ measurement still uncertain, but the direction of the frequency change is such as to remove any deviations at all and to leave only the pure quadrupole interaction. If one uses the deviation of the ratio of the $(\frac{3}{2}\rightarrow\frac{5}{2})$ and $(\frac{5}{2}\rightarrow\frac{7}{2})$ transitions as a measurement of ehH, one finds that the standard deviations are about twice the variation from the 2:3 ratio that is necessary for a pure quadrupole interaction. Further annealing would be most helpful in resolving this uncertainty, but the sublimation of the sample at the elevated temperatures has made further measurements impractical. The numbers for ehH in Table III represent the mean values, and if one includes the uncertainty of the central frequency of the $(\frac{1}{2}\rightarrow\frac{3}{2})$ transitions due to this annealing

TABLE II. Annealing effects on nuclear quadrupole resonance in antimony at 4.2°K.

	Sb^{121}		Sb^{123}	
Annealing	Half-intensity width (kc/sec)	Central frequency (Mc/sec)	Half-intensity width (kc/sec)	Central frequeucy (Mc/sec)
24 h at 350°C	35.4±1.0	11.5273±0.0005	22.1±1.0	6.9980±0.0005
2 h at 560°C	31.0±1.0	11.5278±0.0005	24.0±2.0	6.9983±0.0005
2 h at 582°C	30.1±0.4	11.5289±0.0004	19.6±0.7	6.9996±0.0005

[9] J. S. Badami, Z. Physik **79**, 206 (1932).
[10] V. W. Cohen, W. D. Knight, T. Wentink, and W. S. Koski, Phys. Rev. **79**, 191 (1950).
[11] K. Murakawa and S. Suwa, Phys. Rev. **76**, 433 (1949).

effect it must be concluded that the presence of a hexadecapole interaction has not been demonstrated.

Since the larger magnetic moment occurs for Sb^{121}, and the larger quadrupole moment and nuclear spin occur for Sb^{123}, it is possible to establish directly that the linewidths are predominantly the nuclear dipole interaction. Although the standard deviation of the linewidth measurements is in the hundreds of cycles, the uncertainty due to variations from time constants and signal to noise extends the probable error to about 10% of the linewidth. In the annealing data shown in Table II, the variations in the linewidths shown for the various samples are within this limit of error.

IV. TEMPERATURE DEPENDENCE

The temperature dependence of the interaction has been measured by following the $(\frac{1}{2} \rightarrow \frac{3}{2})$ transition of Sb^{121} from 2 to 480°K. The results of these measurements are shown in Fig. 1; the approximate quadrupole

TABLE III. Measured resonance frequencies and linewidths at 4.2°K.

Resonance	Frequency (Mc/sec)	Half-intensity width (kc/sec)
	Sb^{121}	
$(\frac{1}{2} \rightarrow \frac{3}{2})$	11.5289±0.0004	30.1±0.4
$(\frac{3}{2} \rightarrow \frac{5}{2})$	23.0611±0.0002	16.4±0.2
	Sb^{123}	
$(\frac{1}{2} \rightarrow \frac{3}{2})$	6.9996±0.0005	19.6±0.7
$(\frac{3}{2} \rightarrow \frac{5}{2})$	13.9997±0.0005	10.3±0.2
$(\frac{5}{2} \rightarrow \frac{7}{2})$	21.0000±0.0002	7.5±0.6
	$eqQ_{Sb^{121}}=76.8672\pm0.001$ Mc/sec.	
	$ehH_{Sb^{121}}=+15\pm5^{a}$ kc/sec.	
	$eqQ_{Sb^{123}}=97.9993\pm0.001$ Mc/sec.	
	$ehH_{Sb^{123}}=+13\pm30^{a}$ kc/sec.	

[a] This error is the standard deviation of the measurements. The existence of a systematic error due to crystal imperfections is discussed in the text.

coupling eqQ is readily obtained by multiplying the $(\frac{1}{2} \rightarrow \frac{3}{2})$ resonance frequency by 20/3. A comparison has been made of the temperature dependence of the Sb^{121} and Sb^{123} interactions. Since the $(\frac{3}{2} \rightarrow \frac{5}{2})$ transition of Sb^{123} is near the $(\frac{1}{2} \rightarrow \frac{3}{2})$ of Sb^{121}, these two resonances were measured alternately in the same rf coil and at the same fixed temperatures of 4.2, 78, and 300°K. The resonance frequencies and their ratios are shown in Table IV. To the precision of the measurements, there is no difference in the temperature dependence of the interaction for the two isotopes. In consideration of a Bayer[12] motional averaging, this result is in agreement with the usual coupled oscillator solution for lattice vibrations in ionic and homopolar solids[13] where the lattice vibrations are determined by the masses of both isotopes. The most direct approach to the determination

[12] H. Bayer, Z. Physik **130**, 227 (1951).
[13] M. Born and T. von Kârman, Physik. Z. **13**, 297 (1912).

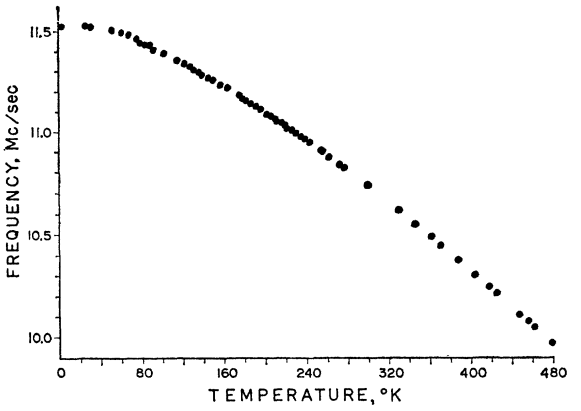

FIG. 1. Temperature dependence of the $Sb^{121}(\frac{1}{2} \rightarrow \frac{3}{2})$ transition.

of the magnitude of the motional averaging would be to repeat these temperature-dependence measurements with an antimony sample of predominantly one isotope. A comparison of the lattice dependence of the ionic field gradient as a function of temperature will be discussed in the next section. The only remaining contribution is a temperature-dependent change of the charge distribution of the extra-ionic electrons. The dependence of these distributions on lattice parameters may be determined by pressure-dependence studies at several temperatures to effect a separation of these lattice-parameter effects from motional effects.

V. ELECTRIC FIELD SOURCES

The first approximation in the calculation of electric field sources in a metal is to assume that the ions are point positive charges and that the extra-ionic electrons form a uniform negative charge background for these ions. The field gradient and the fourth derivative of the field for this model may be calculated very precisely by use of the summing method described in an earlier paper.[14] These sums have been performed,[15] in general, for arsenic-type lattices; applicable results from this work will be used here. Barrett *et al.* have made precision measurements of the antimony lattice parameters at

TABLE IV. Ratio of $Sb^{123}(\frac{3}{2} \rightarrow \frac{5}{2})/Sb^{121}(\frac{1}{2} \rightarrow \frac{3}{2})$.

Temperature (°K)	Freuqencies[a] (Mc/sec)	Ratio
4.2	13.9997 11.5278	1.2144
78	13.9196 11.461	1.2145
300	13.038 10.735	1.2145

[a] The sample used in these measurements was not thoroughly annealed; as a result, the frequencies are different from those in Table II.

[14] R. R. Hewitt and T. T. Taylor, Phys. Rev. **125**, 524 (1962).
[15] T. T. Taylor and E. H. Hygh, Phys. Rev. **129**, 1193 (1963).

TABLE V. eqQ and the ionic field gradient as a function of temperature.

Temperature (°K)	q (ionic sum) $\times 10^{-12}$ esu	eqQ (meas.) (Mc/sec)
4.2	10.15	76.867
78	10.02	76.407
298	10.10	71.613

4.2, 78, and 298°K.[16] Unfortunately, only approximate wave functions are available at this time for Sb^{+++},[17] and no calculations have been completed for the Sternheimer polarizabilities γ_∞ and η_∞; an upper limit can probably be set on $(1-\gamma_\infty)$ at about 15.[18] The measured values of eqQ are compared with the calculated ionic sum at 4.2, 78, and 398°K in Table V. The calculation of the ionic sum has proved to be so sensitive to the lattice parameters that the probable errors in the precision x ray measurements of reference 16 provide an uncertainty in the calculated ionic field gradient that is greater than the temperature dependence of the quadrupole coupling constant in the range of 4.2 to 298°K. The temperature dependence of eqQ and the ionic sum provides no reliable comparison because of this uncertainty. Even the ratios of these two quantities at the three temperatures are not monotonic in their temperature dependence. However, the temperature dependence of the ionic sum is the same order of magnitude as the temperature dependence of eqQ. It appears that the ionic sum accounts for about 10% of the field gradient. The calculation of the remainder of the field gradient must await a calculation of the distribution of the extra-ionic electrons. This calculation can be attempted from a tight-binding approximation, as is often done in a homopolar solid, or from an orthogonalized plane wave (OPW) calculation of the conduction electron density, as has been done for Be.[19]

The calculation of the fourth derivative of the electric field at the ion site by the ionic sum is more defensible than that of the gradient sum, since the only atomic electrons outside of the closed Sb^{+++} shell are the $5s^2$ and $5p^3$, none of them having low enough symmetry to provide a contribution to the hexadecapole interaction. The only other extra-ionic contribution attributable to this interaction is the d character induced by interaction with the d shells of the ion core. This hybridization can be calculated from the OPW method and perhaps from second order effects in a tight-binding approximation.

Since lattice defects have been demonstrated to be accountable for the deviations from pure quadrupole frequencies here, it is important that a further investigation be made of the effect of lattice defects in $SbBr_3$, where hexadecapole interactions have been assigned because of the frequency deviations from a pure quadrupole interaction.[20] If this check demonstrates that the hexadecapole interaction is real, it will provide an excellent differentiation between the extra-ionic electrons of antimony metal and those of that homopolar compound.

ACKNOWLEDGMENTS

The authors wish to thank C. S. Barrett, P. Cucka, and K. Haefner for providing us with the results of their precision lattice measurements in antimony before publication. We also thank T. T. Taylor and Earl H. Hygh for allowing us to use their ionic sum results before publication.

[16] C. S. Barrett, P. Cucka, and K. Haefner (to be published).
[17] E. C. Ridley, Proc. Cambridge Phil. Soc. **52**, 698 (1956).
[18] Private communication with T. P. Das and E. G. Wikner.
[19] M. Pomerantz and T. P. Das, Phys. Rev. **119**, 70 (1960).
[20] T. C. Wang, Phys. Rev. **99**, 566 (1955).